

Research Article

Microbially Induced Calcium Carbonate Plugging for Enhanced Oil Recovery

Chenpeng Song^{1,2} and Derek Elsworth²

¹National Inland Waterway Regulation Engineering Research Center, Chongqing Jiaotong University, Chongqing 400074, China

²Department of Energy and Mineral Engineering, Geosciences, EMS Energy Institute and G3 Center, Pennsylvania State University, University Park, PA 16802, USA

Correspondence should be addressed to Chenpeng Song; songchenpeng@163.com

Received 10 October 2019; Revised 19 March 2020; Accepted 16 June 2020; Published 2 July 2020

Academic Editor: Zhenjiang You

Copyright © 2020 Chenpeng Song and Derek Elsworth. This is an open access article distributed under the Creative Commons Attribution License, which permits unrestricted use, distribution, and reproduction in any medium, provided the original work is properly cited.

Plugging high-permeability zones within oil reservoirs is a straightforward approach to enhance oil recovery by diverting waterflooding fluids through the lower-permeability oil-saturated zones and thereby increase hydrocarbon displacement by improvements in sweep efficiency. *Sporosarcina pasteurii* (ATCC 11859) is a nitrogen-circulating bacterium capable of precipitating calcium carbonate given a calcium ion source and urea. This microbially induced carbonate precipitation (MICP) is able to infill the pore spaces of the porous medium and thus can act as a potential microbial plugging agent for enhancing sweep efficiency. The following explores the microscopic characteristics of MICP-plugging and its effectiveness in permeability reduction. We fabricate artificial rock cores composed of Ottawa sand with three separate grain-size fractions which represent large (40/60 mesh sand), intermediate (60/80 mesh sand), and small (80/120 mesh sand) pore sizes. The results indicate a significant reduction in permeability after only short periods of MICP treatment. Specifically, after eight cycles of microbial treatment (about four days), the permeability for the artificial cores representing large, intermediate, and small pore size maximally drop to 47%, 32%, and 16% of individual initial permeabilities. X-ray diffraction (XRD) indicates that most of the generated calcium carbonate crystals occur as vaterite with only a small amount of calcite. Imaging by SEM indicates that the pore wall is coated by a calcium carbonate film with crystals of vaterite and calcite scattered on the pore wall and acting to effectively plug the pore space. The distribution pattern and morphology of microbially mediated CaCO₃ indicate that MICP has a higher efficiency in plugging pores compared with extracellular polymeric substances (EPSs) which are currently the primary microbial plugging agent used to enhance sweep efficiency.

1. Introduction

Oil has and continues to play a dominant role in global energy systems with various techniques used to enhance its recovery. Typically, oil reservoirs are developed through a series of production stages involving primary, secondary, and tertiary recovery techniques [1]. The successive use of primary then secondary recovery in oil reservoirs may produce only ~20% to ~50% of the original oil in place [2]. Tertiary recovery, also termed enhanced oil recovery (EOR), uses sophisticated techniques to recover oil which is locked within the reservoir and cannot be extracted within the primary and secondary stages of recovery [3]. The purpose of EOR is not only to restore

formation pressure but also to improve oil displacement or fluid flow in the reservoir [4]. The four major types of EOR operations are chemical flooding, gas displacement (miscible flooding and immiscible flooding), thermal recovery (steam-flood or in situ combustion), and microbially enhanced oil recovery [5].

Microbially enhanced oil recovery (MEOR) is a biologically based technology consisting of manipulating the function and/or structure of native microbial environments present in oil reservoirs [6–8]. Specifically, selected microorganisms are capable of metabolizing hydrocarbons producing organic solvents or secreting microbially mediated products which can improve the fluidity of the crude oil or selectively

plug the high-permeability zones of the oil reservoir to enhance sweep efficiency [9, 10]. Sweep efficiency is a term used to measure the extent to which the displacing fluid is in contact with the oil-bearing parts of the reservoir [11] and is one of the critical indicators affecting oil recovery [12]. Heterogeneous reservoirs impede sweep efficiency, since waterflooding fluids are preferentially transmitted through the high-permeability “thief zones” without sweeping through low-permeability oil-saturated zones. Thus, the plugging of the high-permeability thief zones necessarily diverts the waterflood fluids through the lower-permeability oil-saturated zones within the reservoir [13]. This causes the flow to be equally divided between high- and low-permeability layers, so that the waterflood uniformly “sweeps” the reservoir with an improved “sweep efficiency.” Therefore, simple plugging of the high-permeability “thief zones” is the most plausible and also the most straightforward and achievable approach to enhance “sweep efficiency” and thereby improve oil recovery.

In this work, we investigate the feasibility of a biomineralization approach to plug the high-permeability zones of oil reservoirs. Research in biomineralization indicates that certain strains of microorganisms are able to induce calcium carbonate precipitation by enzymatic hydrolysis of urea and bioavailable calcium ions. This bioprocess is often referred to as microbially induced carbonate precipitation (MICP) with *Sporosarcina pasteurii* most commonly employed in MICP [14]. This bacterium can secrete highly active urease in its metabolic process. This enzyme can catalyze the hydrolysis of urea into ammonia (NH_3) and carbon dioxide (CO_2). These hydrolyzed products then diffuse into the solution around the cells and promptly hydrolyze to ammonium (NH_4^+) and carbonate (CO_3^{2-}). When this hydrolysis reaction occurs in the presence of surrounding dissolved calcium ions, the carbonate reacts with calcium ions to form calcium carbonate (CaCO_3) [15–17]. The hydroxide (OH^-) generated from the hydrolysis of urea leads to an increase in pH which provides favorable conditions for calcium carbonate precipitation. As the concentration of calcium carbonate around the bacteria exceeds its saturation point, supersaturated calcium carbonate first transforms into an amorphous precipitate ($\text{CaCO}_3 \cdot \text{H}_2\text{O}$) and then spontaneously transforms into vaterite or calcite with microorganisms as the nucleation sites [18]. *Sporosarcina pasteurii* in the MICP process provides urease for the hydrolysis of urea and also acts as nucleation sites for the crystallization of CaCO_3 . The biochemical process of microbially induced calcium carbonate precipitation is shown in Figure 1. Unlike chemically synthesized calcium carbonate, this microbially mediated calcium carbonate exhibits high cohesiveness and mechanical strength and thus is able to act as a biological clogging agent that reduces the permeability of the porous medium [19, 20]. In addition, *Sporosarcina pasteurii* can endure with strong biological activity in highly alkaline or acidic conditions and high salinity [21]. Thus, this microbial interaction has the potential for selective plugging of high-permeability thief zones.

The following explored the microscopic characteristics of MICP-plugging and its effectiveness in permeability reduction. Specifically, *Sporosarcina pasteurii* was used as the microbial stock for these pore-plugging/occlusion exper-

iments. The aggregates of Ottawa sand comprise three separate grain-size fractions representing large (40/60 mesh sand), intermediate (60/80 mesh sand), and small (80/120 mesh sand) pore sizes to investigate the efficacy and micro-process of MICP-plugging as a result of different biotreatment periods.

2. Materials and Methods

Aggregates of Ottawa sand conforming to three separate size fractions (40/60 mesh, 60/80 mesh, and 80/120 mesh) were used as artificial rock core of variable pore size to examine the effectiveness of MICP on permeability reduction for different durations of microbial treatment.

2.1. Bacteria Cultivation. *Sporosarcina pasteurii* used in this study was obtained from the American Type Culture Collection (freeze-dried, ATCC 11859). The growth medium was the NH₄-YE liquid medium (ATCC 1376). The bacterial cultures were cultured at 30°C in the shaking water bath (200 r/min) for 36–48 h before harvesting at $\text{OD}_{600} = 1.4 - 1.6$. OD_{600} is an abbreviation standing for the optical density of a sample measured at a wavelength of 600 nm. It is a standard measurement method for estimating the concentration of bacterial or other cells in a liquid [22]. The suspended bacteria solution culture was then centrifuged twice at 4000 g for 30 minutes, removing the supernatant liquor and supplementing fresh NH₄-YE growth media after each centrifugation. After the centrifugation process, the bacteria solution was stored at 4°C prior to MICP treatments.

2.2. Artificial Core Set Assembly. The Ottawa sand aggregates were used as the artificial cores to examine the efficacy of MICP treatment. Ottawa sand is a naturally occurring near-spherical near-pure quartz sand recovered from Ottawa, Illinois, and the St. Peter formation [23]. The sand was sieved into one of the three grain size classifications: 80/120 mesh (0.180 mm–0.125 mm), 60/80 mesh (0.250 mm–0.180 mm), and 40/60 mesh (0.425 mm–0.250 mm), which were used as artificial cores reflecting three distinct pore size distributions. The sieved Ottawa sand was soaked in hydrochloric acid solution (5 mol/L) to remove extraneous mineral matter. The materials were then washed in deionized water and dried at 105°C for 24 hours prior to MICP treatment. A cylindrical PVC tube [1 inch (25 mm) in inner diameter and 12 inches (300 mm) in length] was used as the experimental core holder with the sand column 10 inches (250 mm) in length. Each grain-size distribution was prepared into three identical columns for different exposure of the microbial treatments. The initial porosity of the particle aggregate for each size fraction was determined by helium porosimetry. The sample/particle assembly process for the porosity measurement was the same as that for the subsequent MICP experiment which was to cover the sample with a 100 g balance weight and manually vibrate for 1 minute. The measured initial porosity and permeability of the columns are shown in Table 1.

2.3. Column Bead-Pack Flow Assembly and Experimental Procedure. The experimental apparatus was illustrated in Figure 2. The *Sporosarcina pasteurii* suspension, stationary

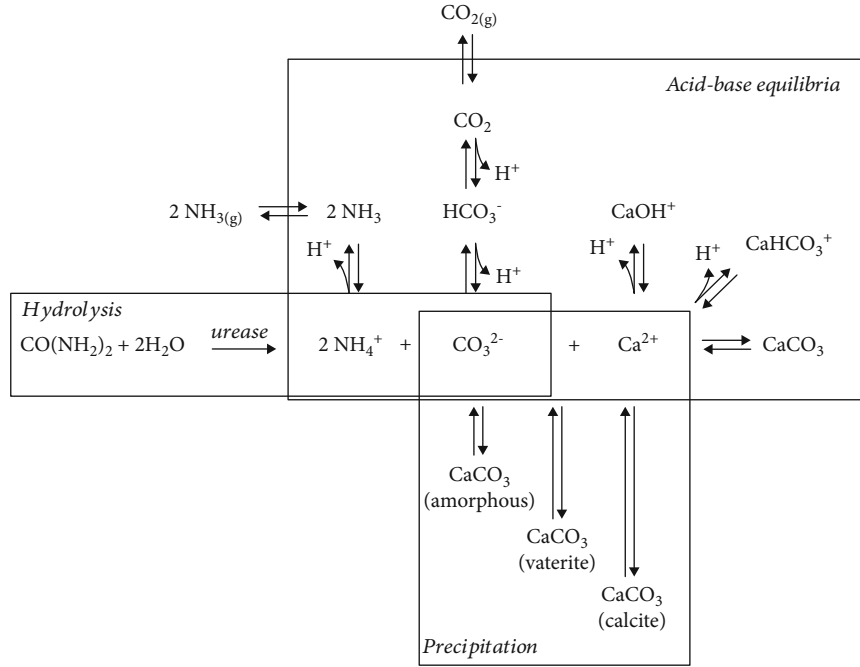


FIGURE 1: The biochemical process of MICP [15].

TABLE 1: Initial permeability and porosity of each core comprising the three grain-size distributions.

Permeability k_0 (Darcy)	40/60 mesh			60/80 mesh			80/120 mesh		
	#1	#2	#3	#1	#2	#3	#1	#2	#3
	15.43	14.74	17.17	2.74	2.34	2.42	1.05	1.12	1.23
Porosity	0.391			0.397			0.388		

liquid (0.05 mol/L CaCl_2), and cementation solution (1.0 mol/L CaCl_2 and 1.0 mol/L urea) were sequentially injected into the sample from the bottom entry of the core holder by a peristaltic pump. Calcium ions in the stabilizing solution can enhance the adhesion of bacteria to the surface of the particles as well as bacterial flocculation [24]. The sand column has a permeable buffer layer at both fluid inlet and outlet with the column sandwiched in-between. A standard injection procedure was as follows:

- 60 ml of the bacterial suspension was first injected into the column at a rate of 0.5 mL/min
- Each sample was then stood for two hours to allow the bacteria to attach to the particle surfaces
- 10 ml of stationary liquid was injected at a rate of 0.50 mL/min
- The last step was injecting 100 ml of cementation solution at a rate of 0.50 mL/min

The steps (a–d) constituted a single MICP-cycle. These sand flow-through columns for all three grain-size distribution were individually performed 4, 6, and 8 cycles of injections to represent various biotreatment durations. The injection was performed continuously, with no interval between the two subsequent cycles.

After MICP treatment, each column is dissected longitudinally into five equal-length segments [2 inches (50 mm) in length] to measure both permeability and calcium carbonate content of each section. The permeability is measured for steady flow based on Darcy’s law [25];

$$k = \frac{QL\mu}{\Delta PA} \quad (1)$$

where k is the permeability, Q is the volumetric flow rate, μ is the dynamic viscosity of the fluid, L is the length of the specimen, ΔP is the pressure difference, and A is the cross-sectional area of the segment.

The calcium carbonate (CaCO_3) content is examined by immersing a small amount of each segment into 5.0 mol/L hydrochloric acid to fully remove the carbonate and then measuring mass difference before and after this treatment. The calcium carbonate content is determined as follows:

$$W_{\text{CaCO}_3} = \frac{M_{\text{sand}+\text{CaCO}_3} - M_{\text{sand}}}{M_{\text{sand}}} \quad (2)$$

where W_{CaCO_3} is the calcium carbonate content, $M_{\text{sand}+\text{CaCO}_3}$ and M_{sand} represent the dry weight of the sample before and after immersing in hydrochloric acid, respectively.

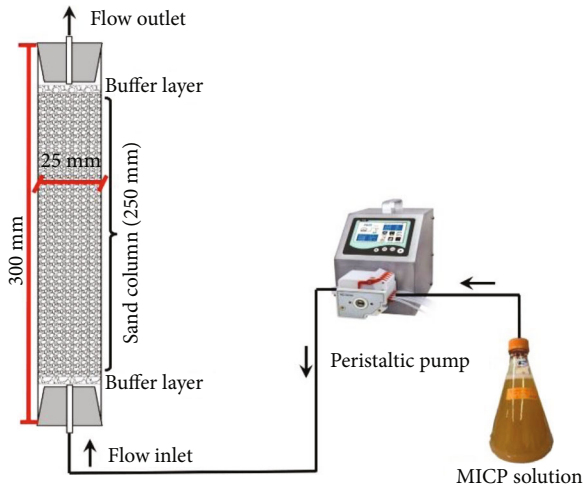


FIGURE 2: Schematic of the experimental arrangement.

3. Experimental Results

Measured permeabilities are shown in Figure 3. Overall, the permeabilities of the samples with the three pore size distributions reduce with an increase in the cumulative nutrient volume injected. Specifically, the permeability of artificial cores containing large pores (40/60 mesh sand) after four, six, and eight cycles of MICP-treatment are 11.39~13.49 D, 9.17~12.18 D, and 7.40~9.92 D, respectively. The permeability of cores containing intermediate-sized pores (60/80 mesh sand) are 1.83~1.96 D, 1.33~1.69 D, and 0.81~1.06 D, while the cores representing the smallest sized pores (80/120 mesh sand) are 0.74~0.92 D, 0.51~0.66 D, and 0.18~0.33 D.

After the permeability test, the calcium carbonate (CaCO_3) content of each segment is examined. The correspondence between calcium carbonate content of each segment and permeability is shown in Figure 4. Overall, CaCO_3 mass content in every pore-size sample-type increases with the number of MICP-treatment cycles. The dimensionless relative permeability (k/k_0) is used to compare the normalized effectiveness of plugging among these three pore sizes of cores, where k_0 represents the initial permeability of the untreated cores. For lower calcium carbonate contents (fewer cycles), the normalized reduction in permeability of the samples for these three pore sizes basically agrees. When calcium carbonate content accumulates to a certain level, the change in permeability of the smaller pore-size samples indicates a greater sensitivity in permeability to an equivalent increase in CaCO_3 mass than that for larger pore-size. This is consistent with a greater reduction in pore throat diameter occurring for the smaller pore throats.

4. Microscopic Analysis

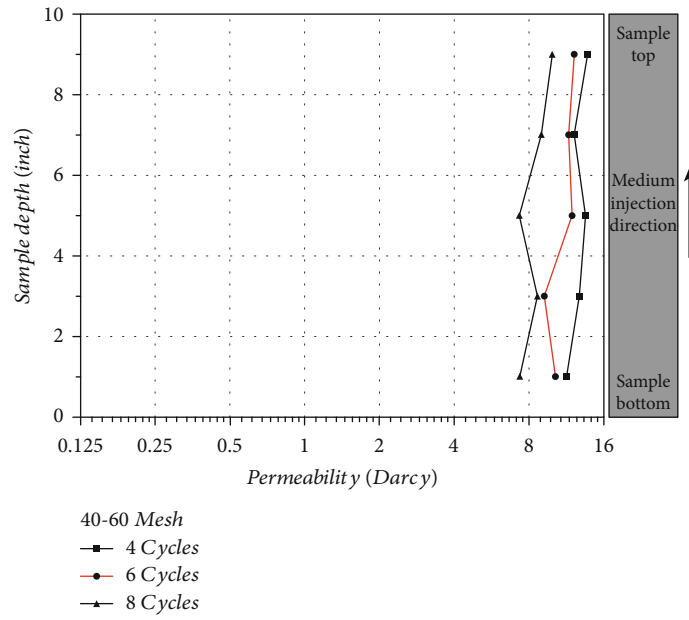
We determine the mineral types comprising the generated calcium carbonate by X-ray diffraction (XRD) of powdered substrates. The microstructure of the deposited calcium carbonate as well as its distribution within the pore space are examined by scanning electron microscopy (SEM) to define microscopic processes of microbially induced plugging.

4.1. Crystal Structure and Distribution of Microbially Induced Calcium Carbonate. As shown in Figure 5, the XRD results indicate that the mineral composition of the biotreated specimens includes quartz, vaterite, and calcite. Quartz is the mineral component representing the Ottawa sand comprising the artificial core. Vaterite and calcite, representing two polymorphs of calcium carbonate, are the microbially produced components. The XRD results also indicate that more than 90% of the calcium carbonate crystals are vaterite. We examine the micromorphology of the generated CaCO_3 as well as its distribution within the pore space using scanning electron microscopy (SEM). As shown in Figure 6, spherical (vaterite) and cubic (calcite) calcium carbonate crystals are generated and irregularly distributed on the particle surfaces. In addition, the particle surfaces are enveloped by a calcium carbonate film.

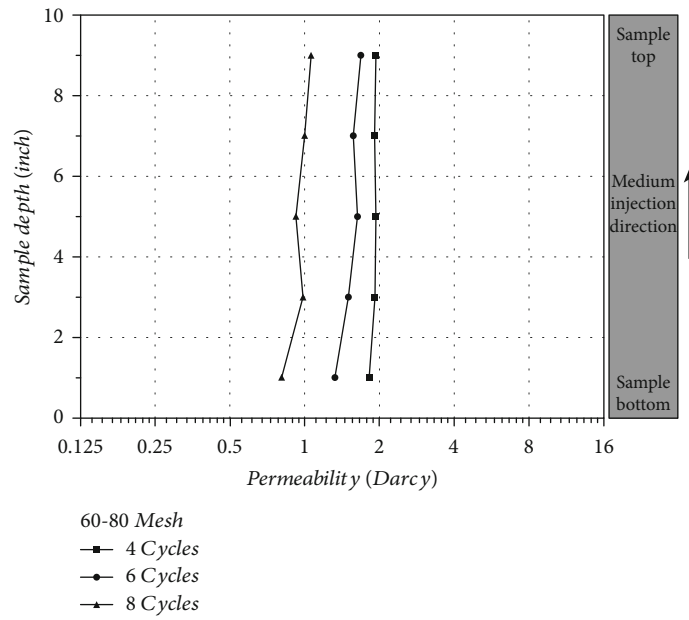
4.2. Processes and Mechanisms of Microbially Mediated Calcium Carbonate Plugging. We characterize the pore-scale microscopic accumulation of CaCO_3 by comparison between SEM images for the 60/80 mesh sand taken after biotreatment for 4, 6, then 8 cycles (Figures 7(a)–7(c)). Both the number and size of the near-spherical calcium carbonate crystals (vaterite) increase significantly with the increasing number of biotreatment cycles, effectively plugging the pore spaces. Based on the SEM images, the mechanisms promoting deposition of biogenerated calcium carbonate in the pore space are described as shown in Figure 8. Microorganisms first adhere to the surface of the particles and gradually induce the production of calcium carbonate with the supply of urea and calcium ions. As the concentration of calcium carbonate around the bacteria exceeds chemical saturation, supersaturated calcium carbonate will transform into amorphous precipitation products which then crystallize with microorganisms as crystal nuclei and form thin layers of calcium carbonate (the process from a to b in Figure 8). With microbially derived calcium carbonate gradually accumulating, some nucleation sites of calcium carbonate crystals will experience further preferential growth, resulting in large, dominant crystals (the process from b to c in Figure 8). As this mass continues to accumulate, the pore spaces are occluded, resulting in a significant decrease in the penetrability of the ensemble medium (the process from c to d in Figure 8).

5. Discussion

In this work, we explored the microscopic characteristics of MICP-plugging and its effectiveness in permeability reduction. This precipitated crystal growth pattern, which is microbially mediated, exhibits a high-efficiency in plugging pore space. The larger pore voids within the artificial core are connected by narrower pore throats, whose connectivity crucially controls the permeability of the ensemble medium. With microbially derived calcium carbonate crystals irregularly occupying the pore spaces, the connection between adjacent pores through these pore throats becomes progressively more tortuous—resulting in a decrease in pore connectivity and therefore permeability. Compared to extracellular polymeric substances (EPSs), which are currently the



(a) 40-60 mesh aggregates



(b) 60-80 mesh aggregates

FIGURE 3: Continued.

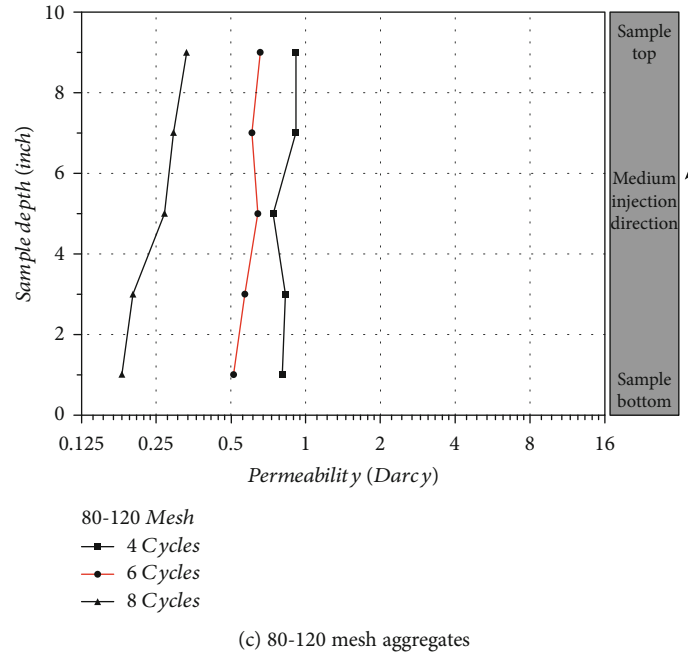


FIGURE 3: Variation in permeability for the treated artificial cores representing (a) 40-60 mesh aggregates, (b) 60-80 mesh aggregates, and (c) 80-120 mesh aggregates for 4, 6, and 8 cycles of nutrient circulation.

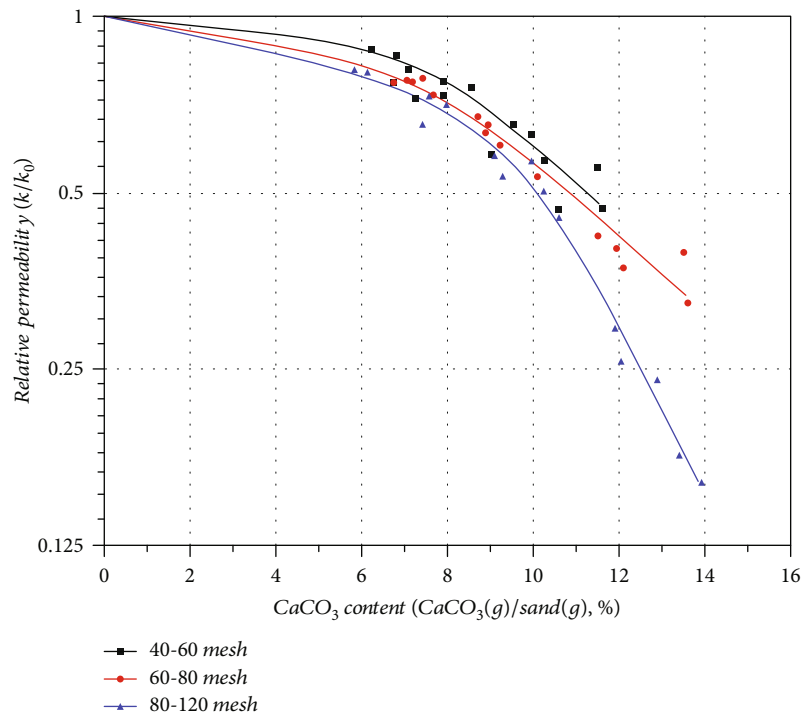


FIGURE 4: Correlation between calcium carbonate content and change in normalized (relative) permeability.

primary microbial plugging agent used to enhance sweep efficiency, biomediated precipitation of CaCO_3 is more effective in plugging in terms of its morphology, size, and growth characteristics. EPSs are high-molecular-weight polymers that are composed of sugar residues and are secreted by a microorganism into the surrounding environment [26].

Although both EPSs and microbially induced carbonate precipitation (MICP) produce microbially mediated products, both have significant differences in substance composition and morphology. EPSs generally maintain a larger surface area and but of a nanoscale thickness (200-1000 nm) [27, 28] (Figure 9), while the single microbial- CaCO_3 crystals

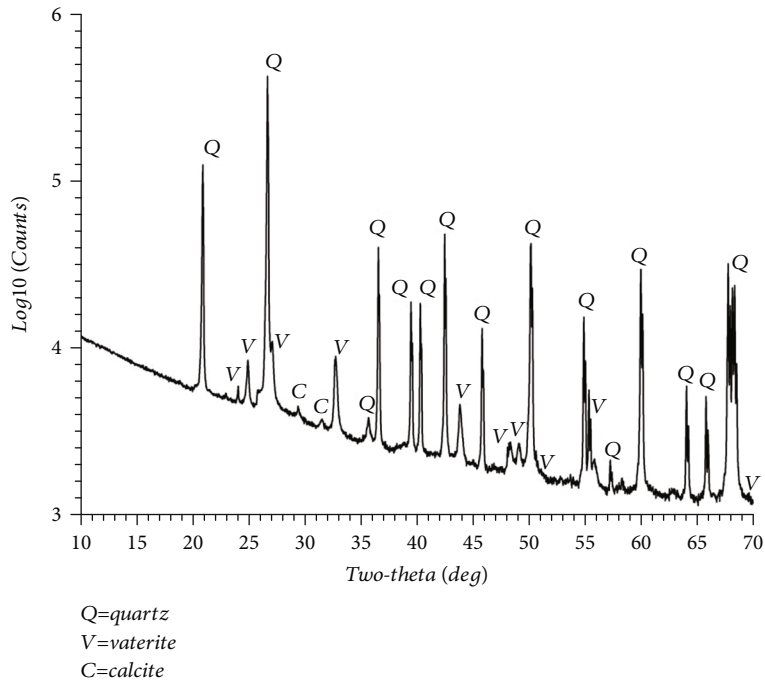


FIGURE 5: Mineral composition of the biotreated sample recovered from X-ray diffraction (XRD).

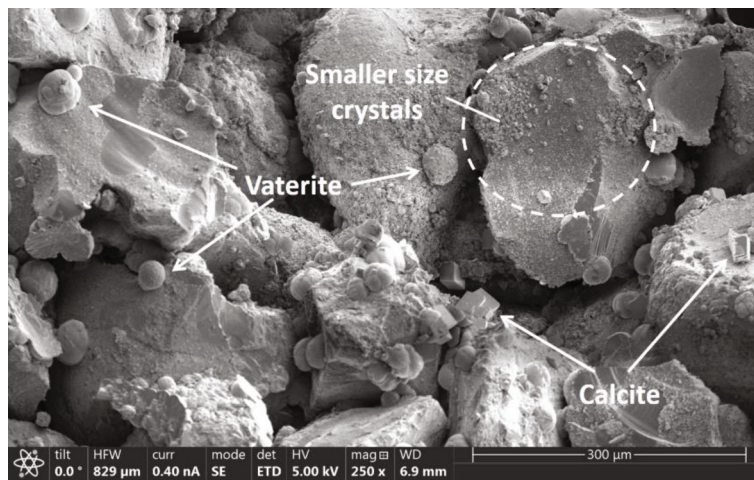


FIGURE 6: Crystal characteristics and distribution of calcium carbonate.

can grow to tens of microns. In terms of the morphology and form of precipitates between EPSs and MICP, the latter appears more effective in plugging pore throats. But this does not necessarily mean that MICP has greater plugging effectiveness than EPSs in practical applications, and many details of MICP still require to be studied.

When MICP is implemented on an engineering scale, the volume of the target formation and the difference in permeability between “thief zones” and the lower-permeability oil-saturated zones should be clarified before implementing MICP—thereby determining the dosage of bacterium/nutrient, transport distance, and treatment duration, so that the bacterial solution can completely sweep through the target area and prevent over-treatment that might transport bacter-

ium/nutrient fluids towards the lower-permeability zones. Therefore, simulating the MICP-implementation process in advance to determine the injection strategy and monitoring the injection flow and pressure during MICP implementation is necessary to achieve accurate plugging for “thief zones.” In addition, this study is only a preliminary demonstration of the potential of MICP as a microbial-plugging agent to enhance the sweep efficiency and does not fully consider that the target is a fractured reservoir. Fractured reservoirs and porous reservoirs are fundamentally different in structure. MICP-plugging exhibits robust plugging effectiveness in porous reservoirs but does not necessarily guarantee high-efficiency plugging in fractured reservoirs. It is clearly necessary to individually investigate the effectiveness and mechanism of

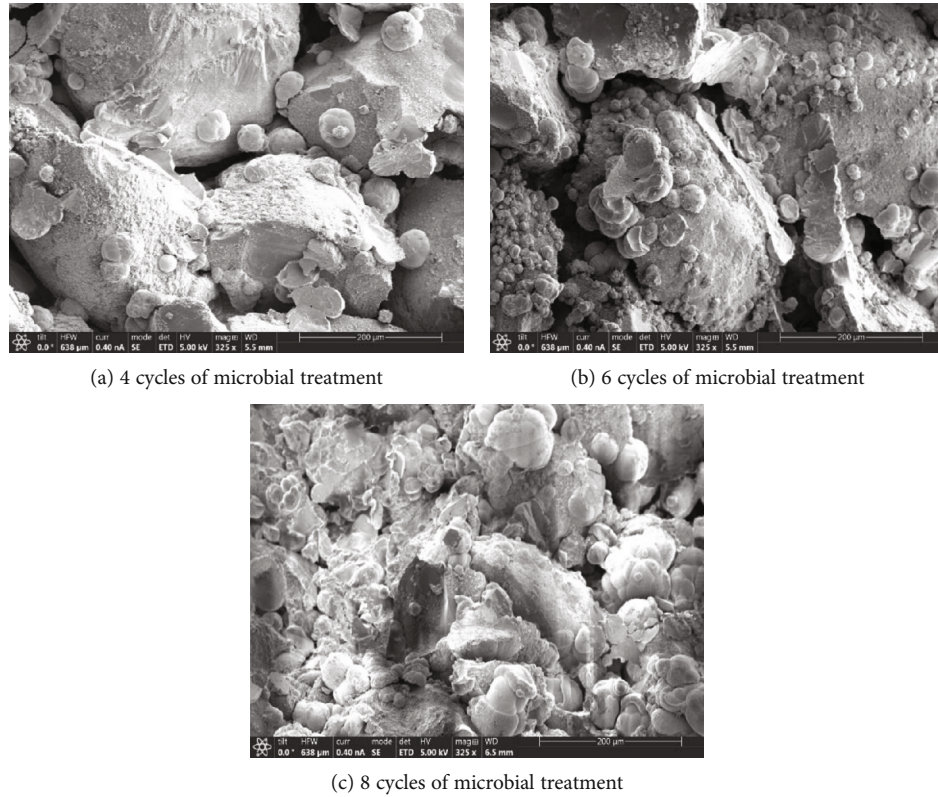


FIGURE 7: Distribution of CaCO_3 within pore space of 60/80 mesh Ottawa sand with biotreated 4, 6, and 8 cycles.

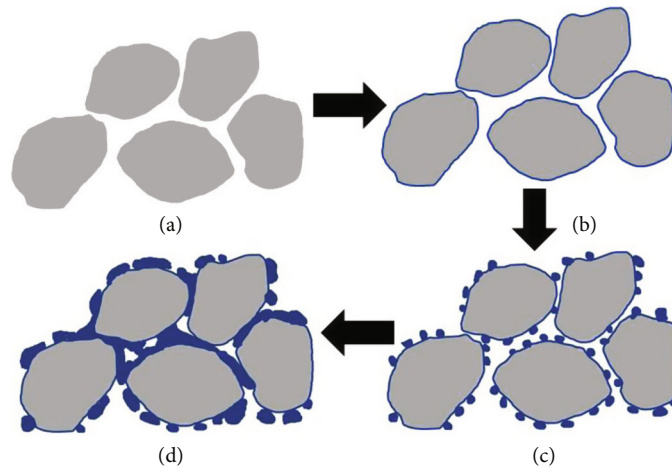


FIGURE 8: Schematic for the cumulative processes of calcium carbonate precipitation within the pore space.

MICP-plugging in fractured reservoirs as a separate topic. The fracture aperture, tortuosity, and initial permeability should be investigated for their influences on the MICP-plugging effectiveness and the microscopic behaviors.

6. Conclusions

Microbially induced carbonate precipitation (MICP) is a biomineralization method for selective plugging of anisotropic oil reservoirs to enhance oil recovery. The experimental results indicate that after eight cycles of microbial treatment

(about four days), the permeability for the artificial cores representing large, intermediate, and small pore size maximally drop to 47%, 32%, and 16% of individual initial permeabilities—suggesting MICP to be a robust effective method for plugging. X-ray diffraction (XRD) indicates that the generated calcium carbonate crystals mainly occur in the form of vaterite. The study reveals the mechanism by which plugging advances. Microorganisms first concentrate on the pore wall where they gradually generate CaCO_3 . As the generated CaCO_3 continuously increases, the pore wall is coated by a thin and largely uniform layer of calcium

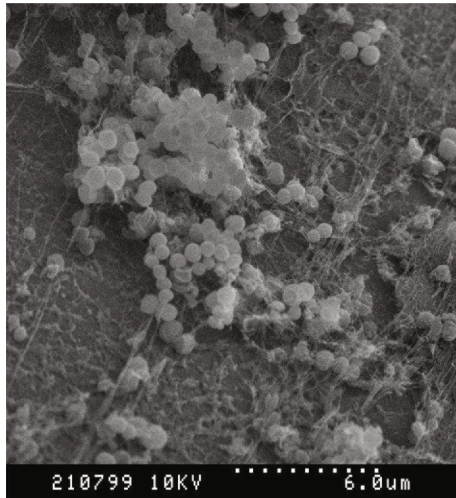


FIGURE 9: SEM image of methicillin-resistant *Staphylococcus pseudintermedius* biofilm formation on 316 L stainless steel orthopedic bone screws. Dotted line = $6\ \mu\text{m}$. Large aggregates of cocci and irregularly produced EPSs are apparent [29].

carbonate. This layer is typically augmented with irregularly distributed crystals of calcium carbonate that act as a plugging agent within the pore space. The connection between the pore throat is interrupted by the microbially derived calcium carbonate crystals, thus resulting in a clear decrease in pore connectivity and ensemble permeability. In terms of the morphology and size of EPSs and MICP, the latter indicates a stronger effectiveness in plugging.

Data Availability

The data that support the findings of this study are available on request from the corresponding author.

Conflicts of Interest

The authors declare that they have no conflicts of interest.

Acknowledgments

This paper is a partial result of support from the National Science Foundation of China (NSFC) under 51604051 and the Natural Science Foundation of Chongqing under cstc2018jcyjA2664. This support is gratefully acknowledged.

References

- [1] E. Tzimas, C. Georgakaki, C. Garcia Cortes, and S. Peteves, *Enhanced Oil Recovery using Carbon Dioxide in the European Energy System*, 2005.
- [2] W. H. Fertl, "Enhanced Oil Recovery, II-Processes and Operations," in *Developments in Petroleum Science*, vol. 17, Elsevier, 1989.
- [3] A. A. Yousef, S. H. al-Saleh, A. al-Kaabi, and M. S. al-Jawfi, "Laboratory investigation of the impact of injection-water salinity and ionic content on oil recovery from carbonate reservoirs," *SPE Reservoir Evaluation and Engineering*, vol. 14, no. 5, pp. 578–593, 2013.
- [4] A. Muggerridge, A. Cockin, K. Webb et al., "Recovery Rates, Enhanced Oil Recovery and Technological Limits," *Philosophical Transactions of the Royal Society A: Mathematical, Physical and Engineering Sciences*, vol. 372, no. 2006, 2014.
- [5] L. N. Nwideo, S. Theophilus, A. Barifcani, M. Sarmadivaleh, and S. Iglauer, "EOR Processes, Opportunities and Technological Advancements," in *Chemical Enhanced Oil Recovery (cEOR) - a Practical Overview*, 2016.
- [6] I. Lazar, I. G. Petrisor, and T. F. Yen, "Microbial enhanced oil recovery (MEOR)," *Petroleum Science and Technology*, vol. 25, no. 11, pp. 1353–1366, 2007.
- [7] R. Sen, "Biotechnology in petroleum recovery: the microbial EOR," *Progress in Energy and Combustion Science*, vol. 34, no. 6, pp. 714–724, 2008.
- [8] K. Fujiwara, Y. Sugai, N. Yazawa, K. Ohno, C. X. Hong, and H. Enomoto, "Chapter 15 Biotechnological approach for development of microbial enhanced oil recovery technique," *Studies in Surface Science and Catalysis*, vol. 151, pp. 405–445, 2004.
- [9] M. Stöckl, N. C. Teubner, D. Holtmann, K. M. Mangold, and W. Sand, "Extracellular polymeric substances from *Geobacter sulfurreducens* Biofilms in microbial fuel cells," *ACS Applied Materials & Interfaces*, vol. 11, no. 9, pp. 8961–8968, 2019.
- [10] C. Caruso, C. Rizzo, S. Mangano et al., "Production and biotechnological potential of extracellular polymeric substances from sponge-associated Antarctic bacteria," *Applied and Environmental Microbiology*, vol. 84, no. 4, 2017.
- [11] J. G. Speight, *Enhanced recovery methods for heavy oil and tar sands*, 2013.
- [12] S. Pingping, Y. Shiyi, D. Baorong, S. Jie, and S. Kuiyou, *Effects of Sweep Efficiency and Displacement Efficiency During Chemical Flooding on a Heterogeneous Reservoir*, SCA, 2005.
- [13] C. Song, Y. Chen, and J. Wang, "Plugging high-permeability zones of oil reservoirs by microbially mediated calcium carbonate Precipitation," *ACS Omega*, vol. 5, pp. 14376–14383, 2020.
- [14] C. Song, D. Elsworth, S. Zhi, and C. Wang, "The influence of particle morphology on microbially induced CaCO_3 clogging in granular media," *Marine Georesources & Geotechnology*, 2019.
- [15] L. A. van Paassen, *Biogrout: Ground Improvement by Microbially Induced Carbonate Precipitation*, Doctoral Thesis, Delft University of Technology, 2009.
- [16] J. T. DeJong, B. M. Mortensen, B. C. Martinez, and D. C. Nelson, "Bio-mediated soil improvement," *Ecological Engineering*, vol. 36, no. 2, pp. 197–210, 2010.
- [17] V. Rebata-Landa and J. C. Santamarina, "Mechanical limits to microbial activity in deep sediments," *Geochemistry, Geophys. Geosystems*, vol. 7, no. 11, pp. 1–12, 2006.
- [18] T. Zhu and M. Ditttrich, "Carbonate Precipitation through Microbial Activities in Natural Environment, and their Potential in Biotechnology: A Review," *Frontiers in Bioengineering and Biotechnology*, vol. 4, 2016.
- [19] C.-X. Qian, A. Wang, and X. Wang, "Advances of soil improvement with bio-grouting," *Rock and Soil Mechanics*, vol. 6, no. 36, pp. 1537–1548, 2015.
- [20] C. Song and S. Liu, "A novel approach of bulk strength enhancement through microbially-mediated carbonate cementation for mylonitic coal," *Geomicrobiology Journal*, 2020.
- [21] C. Song and D. Elsworth, "Strengthening mylonitized soft-coal reservoirs by microbial mineralization," *International Journal of Coal Geology*, vol. 200, pp. 166–172, 2018.

- [22] S. Sutton, "Measurement of microbial cells by optical density," *Journal of Validation Technology*, vol. 17, no. 1, pp. 46–49, 2011.
- [23] S. T. Erdoğan, A. M. Forster, P. E. Stutzman, and E. J. Garboczi, "Particle-based characterization of Ottawa sand: shape, size, mineralogy, and elastic moduli," *Cement and Concrete Composites*, vol. 83, pp. 36–44, 2017.
- [24] D. J. Tobler, J. M. Minto, G. El Mountassir, R. J. Lunn, and V. R. Phoenix, "Microscale analysis of fractured rock sealed with microbially induced CaCO₃ Precipitation: influence on hydraulic and mechanical performance," *Water Resources Research*, vol. 54, no. 10, pp. 8295–8308, 2018.
- [25] J. Wu, X. B. Wang, H. F. Wang, and R. J. Zeng, "Microbially induced calcium carbonate precipitation driven by ureolysis to enhance oil recovery," *RSC Advances*, vol. 7, no. 59, pp. 37382–37391, 2017.
- [26] C. Staudt, H. Horn, D. C. Hempel, and T. R. Neu, "Volumetric measurements of bacterial cells and extracellular polymeric substance glycoconjugates in biofilms," *Biotechnology and Bioengineering*, vol. 88, no. 5, pp. 585–592, 2004.
- [27] U. B. Sleytr, "I. Basic and applied S-layer research: An overview," *FEMS Microbiology Reviews*, vol. 20, no. 1-2, pp. 5–12, 1997.
- [28] K. Czaczyk and K. Myska, "Biosynthesis of extracellular polymeric substances (EPS) and its role in microbial biofilm formation," *Polish Journal of Environmental Studies*, vol. 16, no. 6, pp. 799–806, 2007.
- [29] A. Singh, M. Walker, J. Rousseau, and J. S. Weese, "Characterization of the biofilm forming ability of *Staphylococcus pseudintermedius* from dogs," *BMC Veterinary Research*, vol. 9, no. 1, p. 93, 2013.